STEM CELLS AND DEVELOPMENT
Volume 23, Number 7, 2014

DOI: 10.1089/scd.2013.0362

SEMINAL RESEARCH REPORT

Human and Murine Very Small Embryonic-Like Cells Represent Multipotent Tissue Progenitors, In Vitro and In Vivo

Aaron M. Havens,[1,*] Hongli Sun,[2,*] Yusuke Shiozawa,[1] Younghun Jung,[1] Jingcheng Wang,[1] Anjali Mishra,[1] Yajuan Jiang,[3] David W. O'Neill,[3] Paul H. Krebsbach,[2] Denis O. Rodgerson,[3,†] and Russell S. Taichman[1,†]

The purpose of this study was to determine the lineage progression of human and murine very small embryonic-like (HuVSEL or MuVSEL) cells in vitro and in vivo. In vitro, HuVSEL and MuVSEL cells differentiated into cells of all three embryonic germ layers. HuVSEL cells produced robust mineralized tissue of human origin compared with controls in calvarial defects. Immunohistochemistry demonstrated that the HuVSEL cells gave rise to neurons, adipocytes, chondrocytes, and osteoblasts within the calvarial defects. MuVSEL cells were also able to differentiate into similar lineages. First round serial transplants of MuVSEL cells into irradiated osseous sites demonstrated that ~60% of the cells maintained their VSEL cell phenotype while other cells differentiated into multiple tissues at 3 months. Secondary transplants did not identify donor VSEL cells, suggesting limited self renewal but did demonstrate VSEL cell derivatives in situ for up to 1 year. At no point were teratomas identified. These studies show that VSEL cells produce multiple cellular structures in vivo and in vitro and lay the foundation for future cell-based regenerative therapies for osseous, neural, and connective tissue disorders.

Key Points

HuVSEL and MuVSEL cells are capable of differentiating into multiple germline derivatives in vitro and in vivo.
MuVSEL cells have limited capacity for self-renewal and neither HuVSEL nor MuVSEL cells formed tumors in immunodeficient animals.

Introduction

The regeneration of large and complex tissues resulting from congenital or acquired deficiencies is a significant clinical challenge. Often the clinical needs surpass the tissues available for autologous grafting. Just as challenging is the frequent need for regenerating tissues to form tissues that cross germline boundaries. To this end, numerous approaches have been undertaken utilizing embryonic stem (ES) cells or induced pluripotent stem cells. Each of these approaches has the advantage that large-scale production of transplantable cells is possible, although at significant cost as well as ethical and safety concerns [1–3].

Our group is interested in developing therapies for the regeneration of craniofacial injuries or conditions, which will require the development of multiple tissue components. Previously, we demonstrated that a significant proportion of the osseous regenerative capacity resides in a low-density cellular fraction, which is resistant to agents that induce apoptosis of cells actively undergoing DNA synthesis [4]. Furthermore, this population expresses the G-coupled receptor CXCR4 and therefore migrates rapidly in response to stromal-derived factor-1 (SDF-1 or CXCL12) [5]. Fluorescence activated cell sorting (FACS) further identified very small cells that do not express CD45 or other hematopoietic lineage markers (Lin^-), and in mouse marrow expresses the Sca-1 antigen [6,7]. These small, CXCL12-responsive, $Lin^-Sca\text{-}1^+CD45^-$ cells had previously been described as having embryonic-like features [6,7]. Therefore, the cells were described as very small embryonic-like (VSEL) cells [8,9]. Freshly isolated murine VSEL (MuVSEL) cells, when implanted in vivo, generated mineralized structures with as few as 500 cells, and when transplanted to a bone marrow environment were able to differentiate into adipocytes [5].

VSEL cells represent a rare population in the bone marrow (less than 0.02% of nucleated cells) [10,11]. VSEL cells have been identified in most tissues that have been examined [12], including blood and other solid organs. MuVSEL cells

Departments of [1]Periodontics and Oral Medicine and [2]Biologic and Materials Sciences, University of Michigan, School of Dentistry, Ann Arbor, Michigan.
[3]NeoStem, Inc., New York, New York.
*Contributed equally as first authors.
†Contributed equally as senior authors.

range in size from 3 to 5 μm, while human VSEL (HuVSEL) cells are slightly larger (4–10 μm) [6]. VSEL cells have scant cytoplasm and, as the name suggests, have morphologic characteristics indicative of an immature state of differentiation, including dispersed chromatin [6]. In addition, VSEL cells express genes that are expressed by ES cells, including Oct4, nanog, and stage-specific embryonic antigen SSEA-1 [13]. MuVSEL cells isolated from the marrow express markers characteristic for ES cells, epiblast stem cells, or primordial germ cells [14]. Thus, VSEL cells may give rise to derivatives of all three germ layers [14]. VSEL cells may therefore be prime candidates for cells with the capacity to regenerate many different structures.

The purpose of this study was to determine the capacity of HuVSEL and MuVSEL cells to differentiate into cells that would participate in skeletal repair in vivo. We also sought to determine the extent to which HuVSEL and MuVSEL cells could generate cells of multiple lineages within craniofacial wounds as well as in vitro. The results demonstrate that both HuVSEL and MuVSEL cells are capable of multilineage cellular differentiation in vitro. In vivo, multiple donor-derived tissue lineages, including endothelial cells, neurons, adipocytes, chondrocytes, and osteoblasts, were observed to be derived from MuVSEL cells. Similar tissues were generated from HuVSEL cells. At no point, up to 3 months after transplantation or following three rounds of serial transplantation with HuVSEL or MuVSEL cells, were teratomas observed.

Materials and Methods

HuVSEL cell isolation

HuVSEL cells were isolated from peripheral blood mononuclear cells of healthy Caucasian males following an established mobilization and leukapheresis process. Apheresis products were collected under an IRB approved protocol at NeoStem's laboratory in Cambridge, MA. Each donor received daily injections (480 μg/day) of granulocyte colony-stimulating factor (G-CSF) (NEUPOGEN®; Amgen, Thousand Oaks, CA). Methods for apheresis, elutriation, and FACS sorting of the CD34/CD133$^+$ CD45$^-$ VSEL cells (<10 μm) are provided in the Supplementary Materials and Methods, and Supplementary Fig. S1 (Supplementary Data are available online at www.liebertpub.com/scd). FACS-purified VSELs were typically ~90% pure. FACS-purified VSEL cells were frozen in the NeoStem Laboratory and shipped overnight to the University of Michigan.

MuVSEL cell isolation

MuVSEL (Lin$^-$Sca-1$^+$CD45$^-$ cells) cells were isolated in Ann Arbor from C57BL/6-Tg(CAG-EGFP)131Osb/LeySopJ mice (Jackson Laboratory, Bar Harbor, ME) using a BD FACSAria™ (BD Biosciences, San Jose, CA) as reported previously and see Supplementary Materials and Methods, and Supplementary Fig. S2 [5]. Supplementary Fig. S3 demonstrates MuVSEL cells isolated by FACS and cytospin and stained with an antibody to Oct4 and DAPI nuclear stain.

Induction of hematopoietic stress

C57BL/6 mice (Charles River Laboratories, Wilmington, MA) were bled by jugular venipuncture under a protocol approved by the University of Michigan Committee for the Use and Care of Animals (UCUCA) at the University of Michigan. The mice were anesthetized and ~20%–30% of the calculated blood volume (~0.55 mL for a 20 g mouse) was removed. Control mice were also anesthetized and subjected to puncture without hemorrhage.

MuVSEL and HuVSEL cell culture and differentiation in vitro

HuVSEL and MuVSEL cells were cultured and differentiated as previously described. Briefly, C2C12 cells were cultured in a growth medium (HG-DMEM; Invitrogen, Grand Island, NY) containing 10% fetal bovine serum (Invitrogen) until almost 100% confluent and subsequently treated with 10 μg/mL mitomycin-C (Sigma, St. Louis, MO). HuVSEL and MuVSEL cells were plated at 300–500 cells per well (8-well chamber slide, Lab-Tek) for 1 week. Later, the cells were switched to a differentiation medium (Supplementary Materials and Methods).

Immunofluorescence microscopy

Pepsin treatment of paraffin sections was performed at 37°C for 15 min before application of Image-iT FX signal enhancer (Invitrogen, San Diego, CA) (30 min) and fluorescence-labeled primary antibodies. Poststaining fixation was performed with 10% formalin (Sigma). Slides were mounted with the ProLong Gold Antifade Reagent with DAPI (Invitrogen). Images were taken with the Olympus FV-500 confocal microscope. Antibodies used are presented in the Supplementary Materials and Methods section.

Calvaria defect model

A 3-mm craniotomy defect was established in 5-week-old female SCID mice (CB17-Prkdc^{scid}/LCrlcoCrl) Charles River Laboratories, Raleigh, NC) ($n=10$–12) [15]. Scaffolds (Gelfoam™; Pharmacia & Upjohn, Kalamazoo, MI) loaded with either vehicle or HuVSEL cells were placed into the defects. Mice were sacrificed at 3 months after the implantation. As a positive control, bone marrow stromal cells (BMSCs) from C57BL/6 mice (Jackson Laboratory) were transduced with AdCMVBMP-7 constructed by Cre-lox recombination by Vector Core at the University of Michigan [16,17]. Procedures were approved by the University Committee on the Use and Care of Animals.

Microcomputed tomography

Calvaria were harvested and immediately fixed in 10% neutral buffered formalin for 48 h. The bone specimens were scanned at an 8.93 μm voxel resolution on an EVS Corp., microcomputed tomography (μCT) scanner (London, Ontario, Canada), with a total of 667 slices per scan. GEMS MicroView® software was used to make a 3D reconstruction from a set of scans. A fixed threshold (600) was used to calculate the tissue mineral content.

Serial VSEL stem cell transplantation

Serial transplant studies were performed at intervals of 3 months by injecting green fluorescent protein (GFP)

transgenic MuVSEL (small $Lin^-Sca\text{-}1^+CD45^-$) cells isolated from GFP transgenic murine bone marrow by multiparameter, live sterile cell sorting (BD FACSAria; BD Biosciences)] [14]. Initially, 800 MuVSEL cells were injected intra-tibially and suspended in PBS into 6- to 8-week-old C57BL/6 male mice, which had been exposed to 600 cGray delivered as 300 cGray, 3 h apart. At 3 months, the tibia was flushed and GFP^+ MuVSEL cells were recovered by FACS and reinjected intra-tibially into irradiated secondary (Passage 1) recipient animals. As GFP^+ VSEL cells (small ($<10\,\mu m$) $Lin^-Sca\text{-}1^+CD45^-$ cells) were found in the Passage 1 transplanted animals, secondary (P2) and tertiary (P3) studies were performed by serially transplanting 1,000 GFP^+ ($<10\,\mu m$) cells (See Supplementary Fig. S4).

Real-time polymerase chain reaction evaluations

For gene expression studies, real-time reverse transcriptase polymerase chain reaction (RT-PCR) in conjunction with TaqMan® probes reported to cross intron/exon boundaries was used following reverse transcriptase using primers presented in Table 1. Gene expression was normalized to total murine β-actin or human GAPDH (ABI, Grand Island, NY).

Statistical analysis

Statistical analysis was performed by ANOVA or unpaired two-tailed Student's *t*-test using the GraphPad Instat (GraphPad Software, San Diego, CA) with significance at $P<0.05$. For the μCT analysis, a Kruskal–Wallis test and Dunn's multiple comparisons tests were utilized with the level of significance set at $P<0.05$.

Results

Our goal was first to determine if MuVSEL cells respond to a physiologic wound by rapidly altering their expression of gene sets associated with stem and mature cell markers. Mice were phlebotomized and 2 days later, MuVSEL cells were isolated. MuVSEL cells responded to the acute bleed by decreasing their expression of stem cell markers (SSEA-1, Bmi1, and Oct-4) while more mature cellular markers increased (osteocalcin, collagen type 1, nestin, and PPAR-γ) (Table 2).

Table 1. Real-Time Polymerase Chain Reaction Primers Used in Conjunction with Reverse Transcriptase for Gene Expression

Human primers	
Bmi1	Hs01009250_m1
GAPDH	Hs99999905_m1
KLF4	Hs00358836_m1
Myc	Hs00905030_m1
Nestin	Hs00707120_s1
Oct-4	Hs00999632_g1
PAX6	Hs0108812_m1
Runx2	Hs00231692_m1
SOX2	Hs01053049_s1
SOX9	Hs00165814_m1
Tubulin BIII	Hs00801390_s1
Murine primers	
Bmi1	Mm00776122_gH
GAPDH	Mm99999915_g1
Nestin	Mm00450205_m1
Oct-4	Mm00658129_gH
Osteocalcin	RNAOCN-S23A
PPAR-Gamma	Mm01184322_m1
SSEA-1	Mm00487448_s1

Table 2. MuVSEL Gene Expression Change 48 H After Acute Bleed Stress

	Control	*Bleed*
SSEA-1	1	0.38 ± 0.03^a
Bmi1	1	0.33 ± 0.02^a
Oct-4	1	0.15 ± 0.04^a
Osteocalcin	1	6.40 ± 0.10^a
Runx2	1	1.10 ± 0.13
Collagen 1	1	8.11 ± 0.10^a
PPAR-γ	1	4.61 ± 0.68^a

Gene expression measured by real-time PCR following reverse transcriptase for VSEL cells recovered from the bone marrow of $n=3$ animals following an acute bleed stress showed decrease in stem cell markers, while mature cellular markers increased. Animals injected with saline served as the control. Reverse transcriptase-polymerase chain reaction (RT-PCR) was performed following reverse transcription and the data are normalized against data generated from the saline injected animals, which was set to 1. Data presented as mean ± std. deviation. Significance is indicated by [a] for $P<0.05$.

MuVSEL, murine very small embryonic like.

In vitro differentiation of MuVSEL cells

Table 2 suggests that VSEL cells may differentiate into mature phenotypes following physiologic stimuli. We therefore determined if VSEL cells can generate cells of all three germ layers in vitro. Alone, MuVSEL cells demonstrated very limited proliferation and were unable to differentiate (not shown). MuVSEL cells were therefore isolated from GFP mice and placed on mitomycin-C-treated C2C12 cells. After 2 weeks, the medium was switched to the differentiation medium for up to two additional weeks before histological evaluation (Fig. 1A). Under osteoblastic conditions, many C2C12 cells express Runx2 or osteocalcin, markers indicative of osteoblast differentiation (Fig. 1B). These C2C12 cells could be distinguished from the VSEL cells by their larger nucleus and the lack of GFP expression. At the same time, many of the GFP-expressing VSEL cells strongly expressed Runx2 or osteocalcin (Fig. 1B). Under endothelial conditions, significant expression of Factor VIII and PECAM-1 (CD31) was observed for the GFP-expressing cells (Fig. 1C). When MuVSEL cell/C2C12 cell cocultures were induced toward neural differentiation, nestin and neurofilament 200 expression was observed. In fact, many of the cells exhibited a bipolar and multipolar morphology with cell processes extending away from a central cell body (Fig. 1D). Furthermore, when MuVSEL cells were placed into a endodermal (pancreatic) differentiation medium, insulin and C-peptide expression, was seen following coculture with C2C12 cells (Fig. 1E).

In vitro differentiation of HuVSEL cells

To determine if HuVSEL cells are also able to generate cells from all three germ layers, HuVSEL cells were isolated

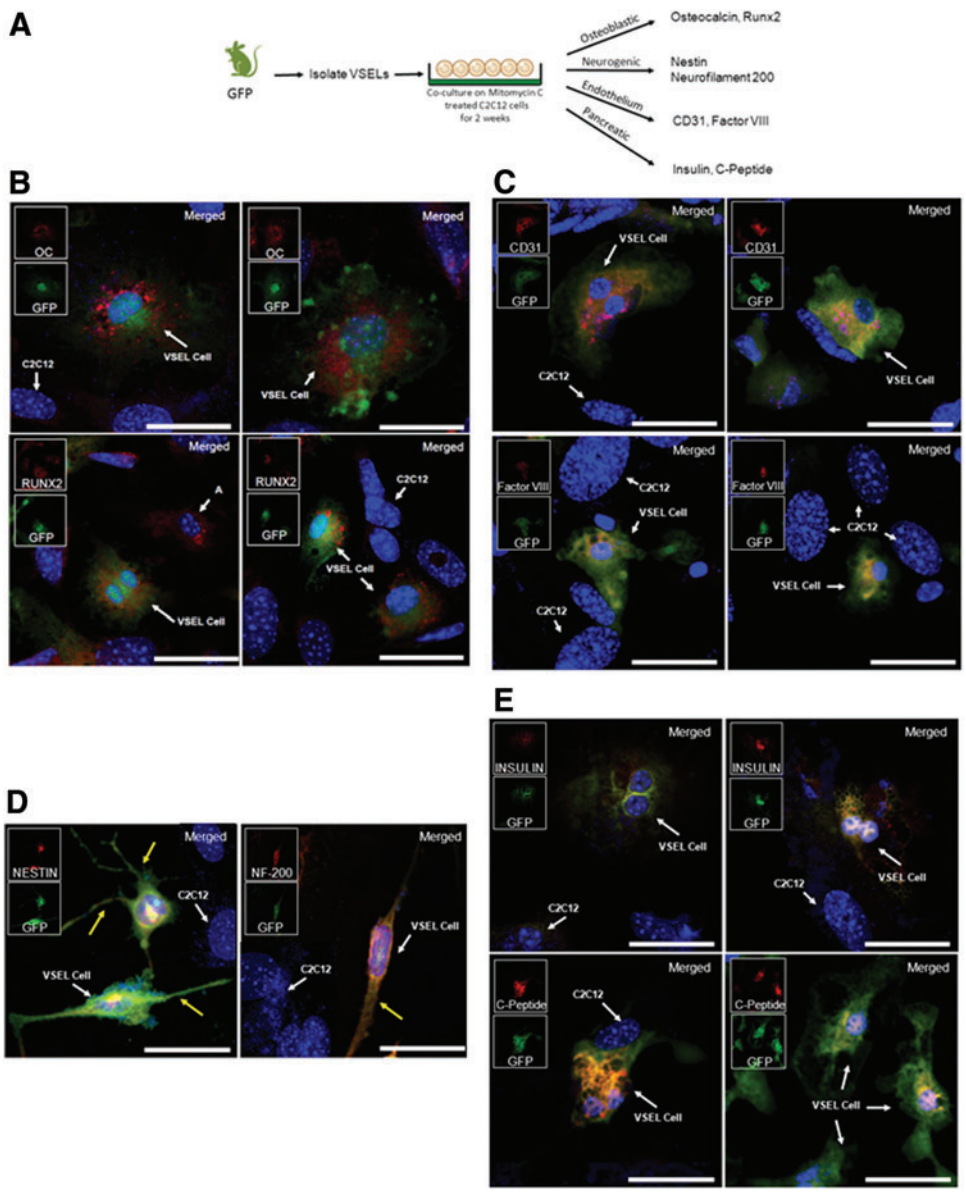

FIG. 1. In vitro MuVSEL cell differentiation into multiple germline tissues. **(A)** In primary culture, MuVSEL cells were freshly isolated from the bone marrow of GFP-labeled animals and cocultured on mitomycin-C-treated C2C12 cells for 2 weeks. Cells were placed in specific differentiation media conditions and were evaluated for expression for **(B)** osteoblastic [osteocalcin (OC) and Runx2], **(C)** endothelium (CD31, Factor VIII), **(D)** neural [nestin and neurofilament 200 (NF-200)]; *yellow arrows* indicate neuron extensions, and **(E)** insulin-producing endodermal (insulin and C-peptide)-specific markers. In each case, colocalization of the specific antibody (OC, Runx2, CD31, Factor VIII, nestin, neruofilament 20 each stained *red*) with GFP (stained *green*) was employed (merged staining appears *yellow*). *Red* and *green inserts* show each single color at 22% size of the merged images. The C2C12 cells did not express GFP, and therefore in combination with any of the aforementioned specific markers represent internal negative controls. (Note a few non-GFP expressing cells did stain for Runx 2 (labeled "A") likely derived from C2C12 cells). *Large panel* immunohistochemistry images presented at 40×, scale bar = 100 μm. GFP, green fluorescent protein; MuVSEL, murine very small embryonic like. Color images available online at www.liebertpub.com/scd

from volunteers following G-CSF mobilization. Initial studies were performed comparing the expression of selected gene markers by G-CSF-mobilized HuVSEL cells to $CD45^+$, $CD34^+$ cells. Like the MuVSEL cells, HuVSEL cells expressed Oct4 and Bmi1 and had lower levels of expression of the mature marker osteocalcin compared with controls (Table 3). Like MuVSEL cells, HuVSEL cells alone had very limited capacity to proliferate when placed into single cell or bulk cultures (10–100 cells/well) (not shown). Therefore, cocultures to induce HuVSEL cell differentiation using mitomycin-C-treated C2C12 cells were used.

The ability of HuVSEL cells to express genes indicative of cells of all three germ layers by QRT-PCR was determined (Fig. 2A). Following differentiation, the cocultures were examined for expression of paired box gene 6 (PAX6), which is required for endodermal pancreatic development

TABLE 3. HUVSEL GENE EXPRESSION

	VESL cells	*$CD34^+$*
OCT-4	10.1 ± 2.35^a	1
SOX2	0.31 ± 0.17^a	1
Bmi1	59.7 ± 21.9^a	1
MYC	0.51 ± 0.30^a	1
KLF4	0.71 ± 0.42	1
RUNX2	0	1
Osteocalcin	0	1

HuVSEL cells were isolated by apheresis from peripheral blood following 3 days of granulocyte colony-stimulating factor mobilization. HuVSEL cell gene expression was evaluated by real-time PCR following reverse transcriptase and normalized to GAPDH expression. These values were compared to gene expression of mobilized peripheral blood $CD45^+CD34^+$ cells isolated from the same subject, which was set to 1.

[a] $p < 0.05$.

HuVSEL, human very small embryonic like.

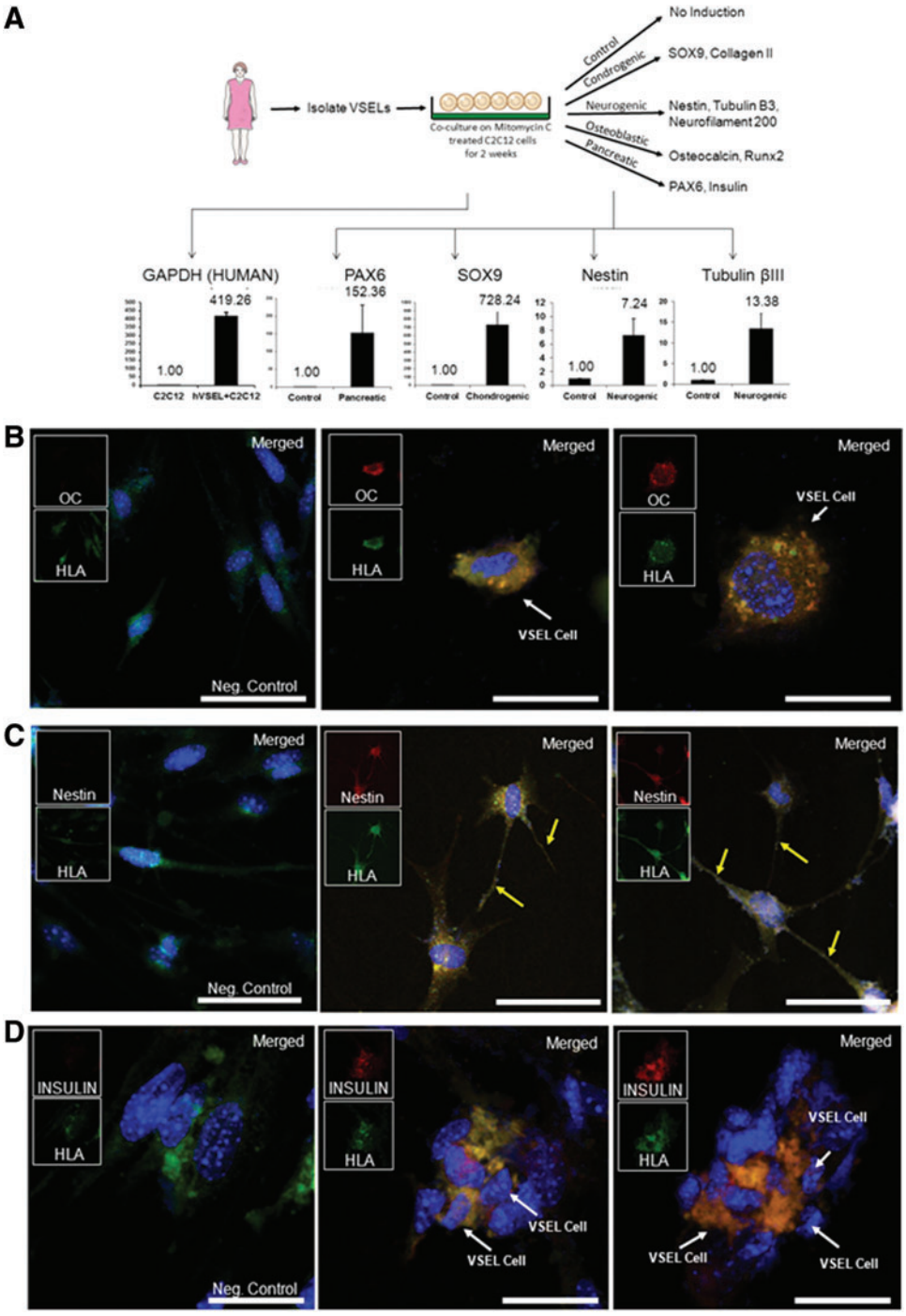

FIG. 2. In vitro HuVSEL cell differentiation into multiple germline tissues. **(A)** In primary culture, HuVSEL cells were freshly isolated from peripheral blood and cocultured on mitomycin-C-treated C2C12 cells for 2 weeks. Expression of human GAPDH by QRT-PCR was over 400-fold higher in cocultures containing HuVSEL cells compared with cultures of C2C12 cells alone (*lower left panel*). After 2 weeks, cells were cultured in specific differentiation media for an additional 2 weeks. Gene expression changes compared with baseline and normalized to GAPDH were evaluated by QRT-PCR for early neural/pancreatic (PAX6), chondrogenic (SOX9), and early neurogenic (nestin and or βIII-tubulin) markers. Cells were also evaluated by immunofluorescence microscopy for expression of **(B)** osteoblastic (osteocalcin), **(C)** early neural (nestin, *yellow arrows* indicate neuron extensions), and **(D)** insulin-producing endodermal (insulin)-specific markers. In each case, colocalization with human HLA staining was assessed. The C2C12 cells did not stain for any of the aforementioned markers. Negative control (Neg. Control) indicates VSEL cells plated on C2C12 without specific tissue induction. *Inserts* show each single color at 22% size of the merged images. *Large panel* immunohistochemistry images presented at 40×, scale bar = 100 μm. HuVSEL, human very small embryonic like; PAX6, paired box gene 6; QRT-PCR, real time reverse transcriptase polymerase chain reaction. Color images available online at www.liebertpub.com/scd

(Fig. 2A, lower left). For mesoderm differentiation, the cocultures were examined for change in the expression of chondrocyte-specific protein SOX9. Ectoderm differentiation was examined with the neural markers nestin or βIII-tubulin. Significant expression of each of these markers was observed in cocultures induced with a pancreatic, chondrogenic, or neurogenic medium (Fig. 2A).

HuVSEL cells were also capable of differentiating into cells that expressed osteocalcin, which is indicative of osteoblastic differentiation (mesoderm) (Fig. 2B). The cells also differentiated into cells that could express nestin in conjunction with the characteristic morphology of neural cells (ectoderm) (Fig. 2C). In other cultures, HuVSEL cells could be induced toward the endodermal pancreatic β-cell lineage as demonstrated by positive staining for insulin (Fig. 2D). In each case, the expression of osteocalcin, nestin, and insulin colocalized with staining for human HLA (Fig. 2B, C, D).

Serial transplantation of GFP transgenic MuVSEL cells

To test the ability of VSEL cells to undergo self-renewal, serial transplants of GFP-labeled MuVSEL cells were

injected into the tibias of locally irradiated mice (Fig. 3A). After 3 months, the tibias were prepared for histology or prepared for FACS analysis to identify GFP-labeled MuVSEL cells. By FACS, ~60% of the VSEL cells maintained their phenotype after the first round of transplants (Fig. 3B and Supplementary Fig. S4). Histology performed on the tibias of passage 1 transplanted animals demonstrated the characteristic morphology and histological locations of GFP-expressing osteoblasts (Runx2), endothelial cells (CD31), early neurons (nestin), and adipocyte (PPAR-γ) cells (Fig. 3C). Peripheral blood of passage 1 mice was examined for cells expressing both the pan-hematopoietic marker CD45

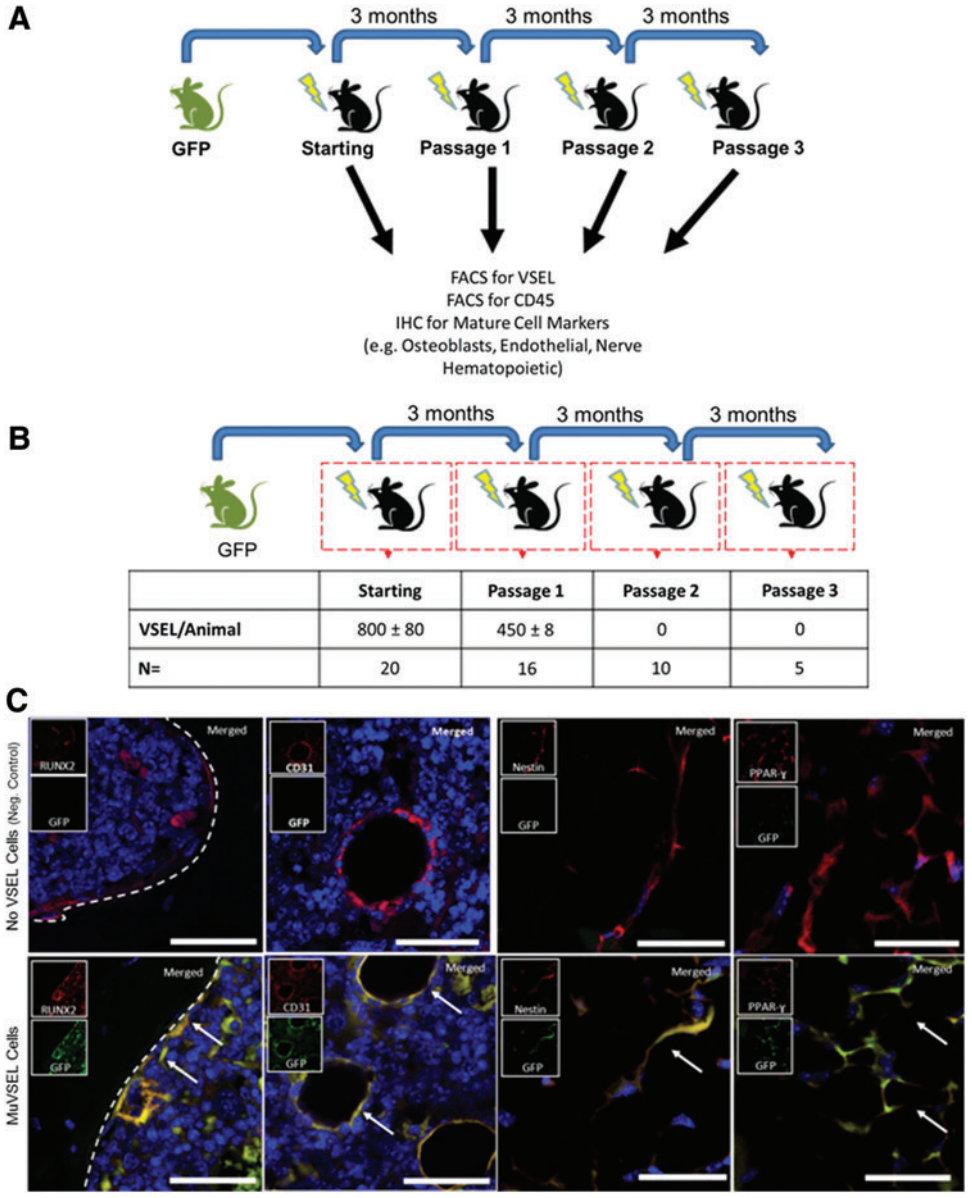

	Starting	Passage 1	Passage 2	Passage 3
VSEL/Animal	800 ± 80	450 ± 8	0	0
N=	20	16	10	5

FIG. 3. Serial transplantation of VSEL cells. **(A)** Serial transplant studies were performed by injecting GFP-labeled VSEL cells into the tibias of locally irradiated mice. Three months after each transplant, mice were sacrificed and the presence of GFP-derived VSEL cells and mature cellular lineages was evaluated by FACS and immunofluorescence microscopy of serially sectioned tibias. FACS **(B)** indicated that ~60% of the number of GFP^+ VSEL cells (small $Lin^-Sca\text{-}1^+CD45^-$ cells) transplanted could be recovered after the first serial transplant from the injected tibia (Passage 1), but no GFP^+ $Lin^-Sca\text{-}1^+CD45^-$ cells could be recovered after subsequent transplants (Passage 2 and Passage 3). Second and third serial transplant data (mice were transplanted with small GFP^+ $CD45^-$ $Sca\text{-}1^-$ cells) indicated that although GFP^+ VSEL cells could not be isolated, abundant GFP^+ cells could be identified by FACS remained at the site of injection. **(C)** Characteristic morphology and histologic locations of GFP-expressing osteoblasts (Runx2), endothelial cells (CD31), neural stem or progenitor cells (nestin), and adipocytes (PPAR-γ) were observed in the P1 mice suggesting that many of the donor MuVSEL cells had differentiated. Note: the brightness nestin-negative control *insert panel* was increased by 30% for visibility. *Inserts* show each single color at 22% size of the merged images. *Arrows* indicate dual staining cells. *Large panel* immunohistochemistry images presented at 40×, scale bar = 100 μm. FACS, fluorescence activated cell sorting. Color images available online at www.liebertpub.com/scd

and GFP. In some cases, extremely low levels of $CD45^+$ cells in the peripheral blood of the transplanted animals also were GFP^+ suggesting that the transplanted VSEL cells may have undergone differentiation into hematopoietic lineages (not shown). No GFP-labeled $CD45^+$cells were identified in the blood of sham-transplanted animals (not shown). At the completion of the second transplants, no VSEL (small $Lin^-Sca\text{-}1^+CD45^-$) cells were isolated, and therefore, only GFP-expressing $CD45^-$ cells were subsequently transplanted. As in the second round of transplants, abundant GFP-expressing cells were observed (not shown), but no VSEL cells were recovered (Fig. 3B). Together, these data suggest that VSEL cells, under the conditions of our assay, have a limited capacity for self-renewal.

In vivo differentiation of HuVSEL cells in a mouse bony defect model

To evaluate the possibility that HuVSEL cells are able to generate osseous tissues in vivo, HuVSEL cells were implanted into calvarial defects in SCID mice (CB17-$Prkdc^{scid}$/LCrlcoCrl), and microcomputed tomography and histological studies were performed. Implantation of 2,000 HuVSEL cells produced robust mineralized tissue by 3 months. Significantly, woven bone was identified within the calvarial defects (Fig. 4A), as well as when the cells were implanted subcutaneously (not shown), compared with animals implanted with collagen scaffolds alone (Fig. 4A). Significantly more bone mineral content was observed in the calvarial defects of VSEL-treated animals relative to cellular or scaffold controls (Fig. 4B). Woven bone formation and a hematopoietic marrow were also observed within the calvarial defects (Fig. 4C). Interestingly, when the HuVSEL cells were implanted in subcutaneous spaces, significant mineralized tissue was also formed demonstrating that the transplanted cells could generate bone, or induce new bone formation, independent of being placed in a bony site (Fig. 4A, B). Antibodies to human HLA demonstrated that the newly generated tissues were of human origin (Fig. 4D). Human-specific osteocalcin and RUNX2 staining along the bone margins were observed indicative of osteoblast differentiation (Fig. 4E).

A histologic examination of the calvarial defects isolated areas of cells surrounded by matrices reminiscent of cartilage was observed. Staining of tissue for collagen type II, which is specifically produced by chondrocytes, colocalized with human-specific HLA staining (Fig. 4F). Robust staining of cells surrounding the lumens of vascular structures was detected with antibody to human CD31, indicating endothelial cells of human origin (Fig. 4F). Staining for nestin identified cells with long processes between cell bodies, suggesting early neuronal commitment (Fig. 4F). Human-specific antibody to PPAR-γ identified adipocytes present within the calvarial defects (Fig. 4F). In each case, no human-specific staining was present in the calvarial defects of cellular or scaffold control treated animals (Fig. 4F). Since HLA staining was seen in the bone marrow (Fig. 4D), we explored whether HuVSEL cells, which had undergone differentiation to the hematopoietic lineage peripheral blood of HuVSEL cell transplanted animals, were examined by FACS; however, the level of cells expressing human CD45 was at or below the level of detection (data not presented). Together these data suggest that HuVSEL and MuVSEL cells have the capacity to generate multiple tissue lineages within an osseous wound, indicating VSEL cells function as multipotent cells.

Tumor formation

Long-term safety is of prime concern when we consider future studies in humans. The ability to generate teratomas is often considered to be one of the hallmarks of pluripotency, yet a concern when potentially used in patients. Teratomas or other tumors were not observed in any of the CB17-$Prkdc^{scid}$/LCrlcoCrl VSEL cell-implanted animals (Table 4).

Since all our prior studies were performed in skeletally mature animals, a subcutaneous ossicle model to implant VSEL cells in rapidly developing or recently matured bone was chosen. In the first group, GFP-bone ossicles were established s.c. in SCID mice by implanting murine BMSCs infected with AdBMP7. At 1 month, the ossicles were exposed and VSEL cells isolated from GFP-expressing mice were injected into the ossicles and followed for 1 year (Fig. 5A, Top). In the second group, VSEL cells were again isolated from GFP-expressing mice and in this case, they were coinjected with BMSCs infected with AdBMP7. As before, these animals were followed for 1 year (Fig. 5A, Bottom). A final control group was established using BMSCs infected with AdBMP7, but these were not exposed to VSEL cells, which expressed GFP. At the time of sacrifice, necropsy identified no tumors at any site in any of the mice. Abundant GFP staining was seen in the marrow and bone structures of the recovered ossicles (Fig. 5B), suggesting that many of the progeny of the VSEL cells remained within the confines of the engineered tissue. Interestingly, more GFP staining was observed in the ossicles in which the VSEL cells had been coimplanted with the AdBMP-7 transduced BMSCs. Critically, no neoplastic tissues were identified in the ossicles (Table 4).

Discussion

In the present report, we evaluated the ability of HuVSEL and MuVSEL cells to give rise to mature cells in vitro and in vivo and correlated this to gene expression and synthesis of proteins from multiple germlines. We observed that both HuVSEL and MuVSEL cells can be induced to express markers that are consistent with the acquisition of osteoblastic (Runx2, osteocalcin), adipocytic (PPAR-γ), and endothelial phenotype (CD31, Factor VIII) cells that are mesenchymal derivatives. Expression of insulin and C-peptide was observed when HuVSEL and MuVSEL cells were placed in a medium that induces mesodermal differentiation. When induced toward neural differentiation, nestin and neurofilament 200 expression was observed by cells that were unipolar, bipolar, and multipolar with cell processes extending away from a central cell body. When HuVSEL cells were implanted into a cranial wound defect, woven human bone was generated with marrow cavities. Contained within the marrow spaces of the human bone, human neural adipocytes, chondrocytes, and osteoblasts

were identified. When MuVSEL cells isolated from GFP-expressing mice were injected into the tibiae, colocalization of either osteoblastic, neural, or blood vessel markers was observed with GFP. Serial transplant studies using MuVSEL cells demonstrated that the donor cells were able to differentiate into cells that expressed RUNX2, CD31, nestin, or PPAR-γ; however, no VSEL cells were recovered after the second round of transplants nor did the cells generate teratoma-like structures even after 1 year. Together the results of the primary and secondary transplants suggest that under the conditions of our assays, donor VSEL cells have limited self-renewal capacity. Together these studies suggest that VSEL cells are worthy of further investigation for clinical regenerative therapies in osseous, neural, and connective tissue disorders.

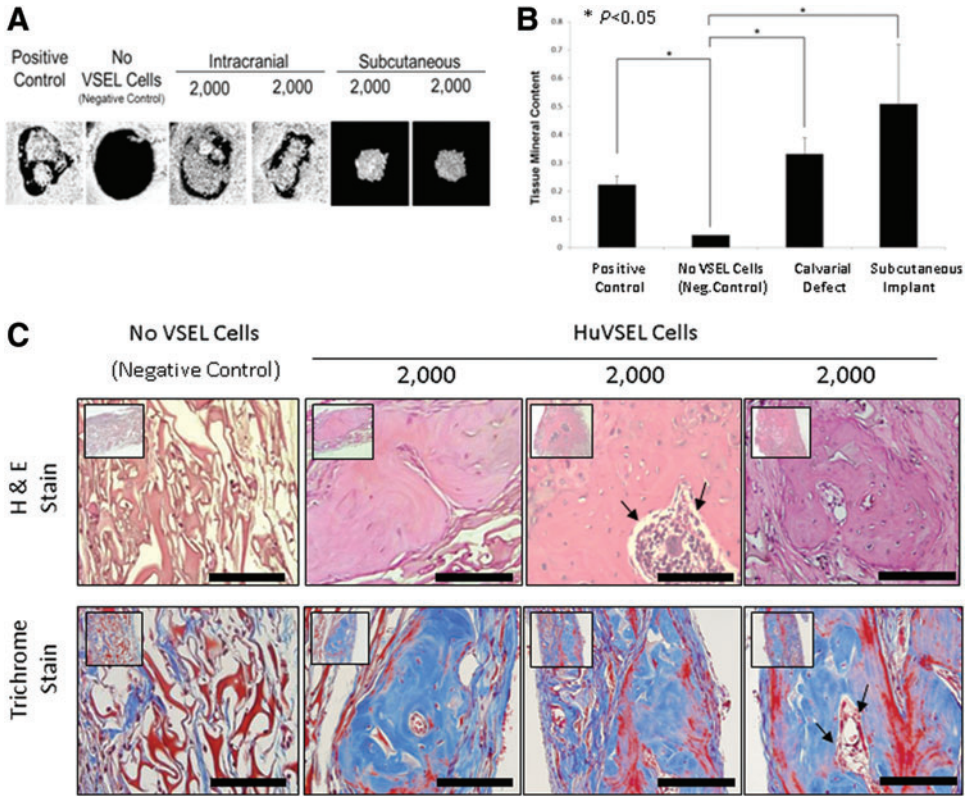

FIG. 4. HuVSEL osseous repair of craniofacial defects. **(A)** Microcomputed tomography images of representative calvarial defects. HuVSEL cells together with collagen carrier matrix were implanted into either calvarial defects (*center panels*) or subcutaneously (*right panels*) at 2,000 HuVSEL cells/implant. Murine bone marrow stromal cells (BMSCs) transduced with AdCMVBMP-7 were implanted as a positive control (*left panel*). Collagen carrier alone was used as a negative control (*second from left*). When implanted both in calvarial defects and subcutaneously, 2,000 BMP-7 BMSCs and HuVSEL cells produced mineralized tissue, whereas collagen carrier alone did not. **(B)** Tissue mineral content for each implant was averaged for $n = 5–7$ animals. Controls and implanted cell numbers were the same as in **A**. Implants using HuVSEL cells or BMP-7 BMSCs produced significantly more tissue mineral content than implants using collagen carrier alone ($^*P < 0.05$). **(C)** Representative sections of calvarial defects stained with H&E (*top row*) and Masson's trichrome (*bottom row*, which stains both collagen and bone blue). Histology is shown at 20× (*inserts*) and 40× magnification. Positive controls were implanted with murine BMSCs expressing BMP-7 (not shown). Negative controls (*left panels*) were implanted with collagen carrier alone (eg, no VSEL cells). Note the persistence of the collagen carrier matrix in the negative control group as well as the absence of an inflammatory cell infiltrate. Implants with 2,000 HuVSEL cells demonstrated woven bone containing marrow spaces (*arrows*). Scale bar = 100 μm. **(D)** Immunostaining of implanted calvarial defects using a fluorescent antibody to human HLA. **(E)** Immunostaining for human-specific antibody to osteocalcin (OC) and Runx2 (both in *red*) merged with images of antinuclear stain (DAPI). *Top left panel* shows negative controls (Neg. Control: implanted with collagen vehicle only, but no VSEL cells) exhibiting no osteocalcin or Runx2 staining. In contrast, tissue sections of HuVSEL implants show significant osteocalcin and Runx2 staining along the bone margin as well as in the marrow cavity. *Arrows* indicate positive cells. *Inserts* show each single color at 22% size of the merged images. *Large panel* immunohistochemistry images presented at 40×, scale bar = 100 μm. *Dashed white line* outlines the bone margins. **(F)** H&E staining of tissue sections (*top row*) show morphologically characteristic cartilage, endothelial, and adipose tissue within the calvarial defect. Immunostaining of defects implanted with HuVSEL cells (*bottom row*) shows robust staining for collagen type-II colocalized with human HLA (*left panel*, identifying chondrocytes) as well as staining surrounding the lumens of vascular structures detected with antibody to human CD31 (*second from left*). Human-specific antibody to PPAR-γ (*second from right*) identifies adipocytes within the calvarial defects. Staining for human nestin (*right*) identified cells with long processes between cell bodies, indicating early neuronal differentiation. In each case, no human-specific staining was present in the calvarial defects of cellular or scaffold control treated animals (*center row*). (Neg. Control: implanted with collagen vehicle only, but no VSEL cells) Histologic images presented at 40×, scale bar = 100 μm. *Arrows* indicate positive staining. Color images available online at www.liebertpub.com/scd

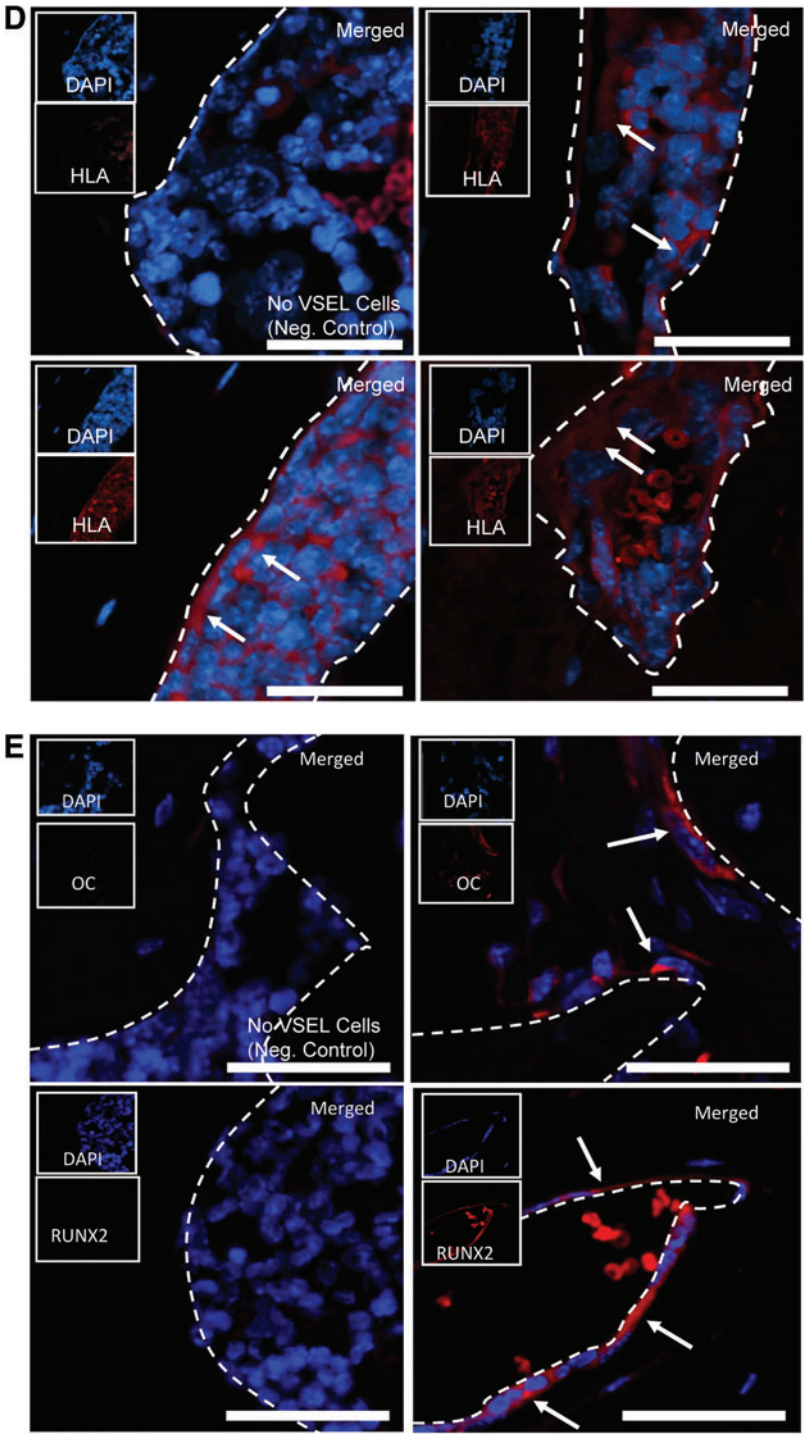

FIG. 4. (Continued).

To our knowledge, this report represents the first demonstration that HuVSEL cells are able to differentiate into multiple cell lineages in vivo and in vitro [6,18,19]. Thus, our data represent an advancement for the field. Previously, we demonstrated that HuVSEL and MuVSEL cells are able to generate osteoblasts in vitro following implantation into osseous wound sites or when implanted in *s.c.* site. It is true that our studies cannot exclude the possibility that a small fraction of hematopoietic cells were carried over in our HuVSEL cell preparations, even with CD45 exclusion. It is possible therefore that some of the activities may have been due to a low level of contaminating cells. However, since the level of engraftment of human CD45 was less than 1%, this possibility appears very unlikely (data not presented), particularly since the animals were not specifically prepared for engraftment by radiation therapy.

It is also true that our studies were not performed with single cell engraftment nor did we perform nuclear tracking

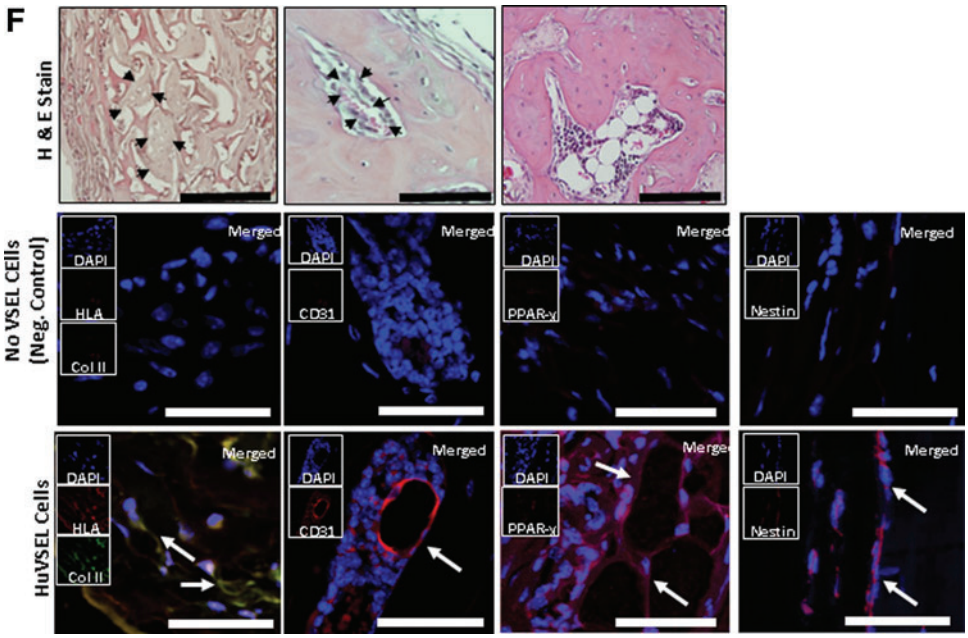

FIG. 4. (Continued).

studies. Numerous reports have demonstrated that cell fusion may play a significant role in the transdifferentiation of cells [20–23]. Therefore, we cannot formally exclude the possibility of cellular fusion. However, if fusion played a significant role in the induction of the mature phenotypes that we observed in culture, we would have seen multiple cells with nuclei that were closer in size to the larger C2C12 nuclei. Therefore, one of the criteria for demonstrating differentiation in our in vitro cultures into any of the lineages we observed was a cell with a smaller nucleus. Moreover, while C2C12 can differentiate into osteoblastic and mesenchymal lineages [24–27], the ability of these cells to activate an endodermal (pancreatic β-cell) or neural (nestin or neurofilament 200) phenotype is unlikely. In addition, it is unlikely that a fused cell in vivo would continue to express human HLA to the levels we observed. Nevertheless, formal proof that cell fusion did or did not play a role in our studies will require further investigation.

Recently, several groups have reported that they have been unable to isolate VSEL cells and suggest that there are insufficient animal data to warrant human clinical trials [28–30]. There is no doubt that isolation of VSEL cells and their cultivation is a difficult endeavor. Given that several independent groups can isolate VSEL cells and have confirmed the in vitro differentiation data [18,31–33], we believe that the reasons for the differences in experimental results are of a technical nature. These differences that are outlined in great detail in a recent publication are most likely due to inadequate isolation procedures [34–36]. Nevertheless, some of the critiques of the VSEL cell field are valid; more systematic studies are needed.

At no point did we observe any evidence for teratoma formation in any of the experimental animals, either at the site of injection or at a distant location. Teratoma formation has been used as part of the criteria that have been established to define pluripotency of ES cells. In fact, VSEL cells fail to contribute to the development of chimeric embryos when injected into blastocysts. We speculate that part of the reason for the failure of VSEL cells to fulfill all of the functional criteria used to define pluripotency may be that the cells have undergone genomic imprinting to limit the ability of the cells to undergo unregulated growth. Yet, MuVSEL and HuVSEL cells express numerous markers associated with a stem cell phenotype, including Oct4 and Bmi1 [37]. Moreover, in vivo we observed the development of tissues derived from HuVSEL cells, including bone, cartilage, blood vessels, fat, and nerve-like structures as well as the formation of a marrow cavity complete with $CD45^+$ expressing cells. Thus, HuVSEL cells fulfill many of the criteria of multipotency in vivo by generating tissues consistent with derivatives from two out of the three germlines within a cranial wound.

These studies did not demonstrate unlimited capacity of MuVSEL cells to self-renew using serial transplantation methodologies. There are several possible reasons for these observations. (i) In the first round of serial transplantation studies, we implanted equal numbers of GFP-labeled MuVSEL cells into the tibia of sublethally irradiated and nonirradiated mice (not shown). As recovery of the GFP-labeled VSEL cells was lower than expected, but was slightly higher for the irradiated group, we continued the studies focusing on the irradiated group exclusively. In retrospect, this was likely a mistake as the wounding process itself likely placed selective pressure on the VSEL cells to undergo differentiation rather than self-renewal. (ii) A second possibility is that, the VSEL cells migrated away from the tibia. Previously, it was demonstrated that human cell or DNA is present in the peripheral blood of animals implanted with HuVSEL cells [15], and that VSEL cells can contribute to hematopoietic reconstitution [38]. Thus, it is possible that the transplanted VSEL cells migrated away from the site of implantation although a careful and more extensive survey of the host tissues would be required. (iii) It is also possible that the results we observed during the recovery of VSEL

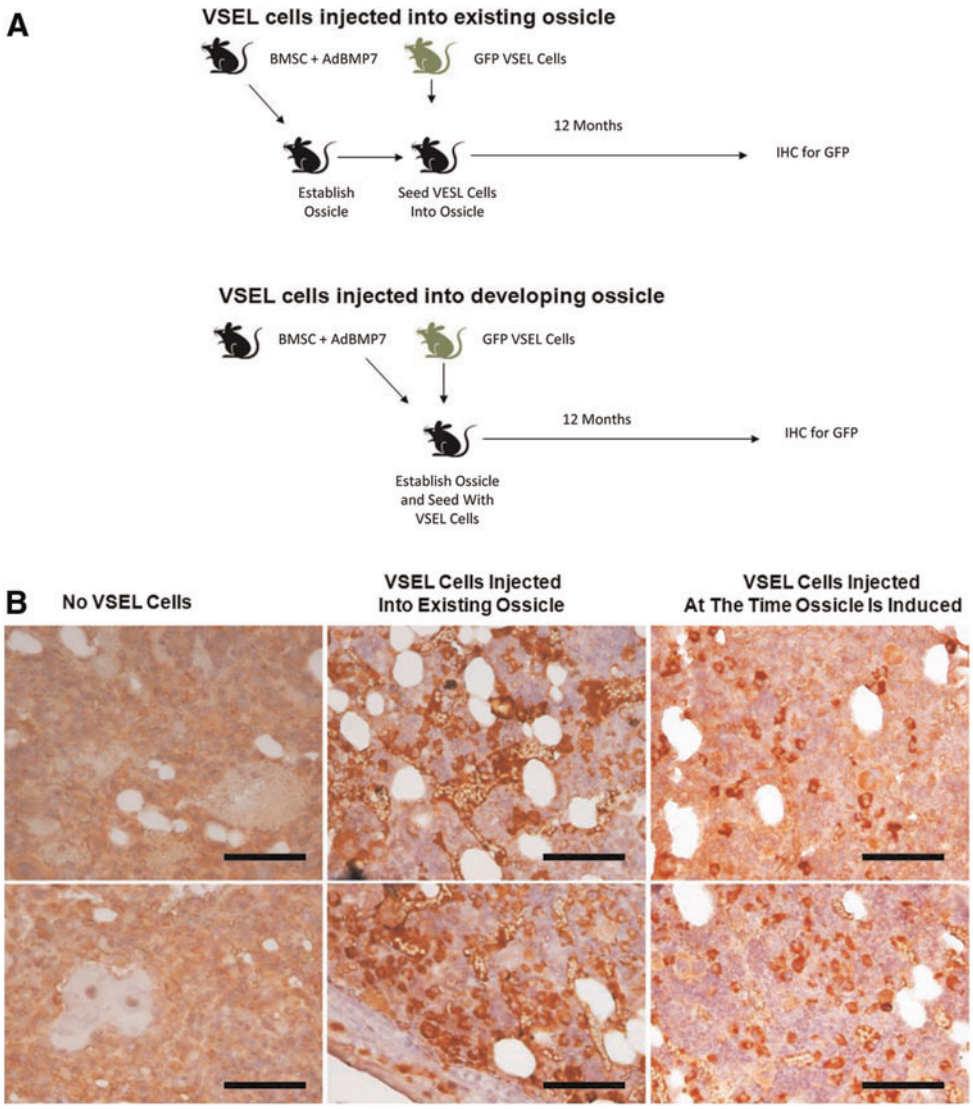

FIG. 5. Long-term subcutaneous ossicle implantation of MuVSEL cells. **(A)** Experimental Outline. *Top:* Murine BMSCs were infected with an adenovirus designed to overexpress BMP7 (AdBMP7), which were then implanted s.c. into SCID mice for up to 1 year. In some cases, the resulting ossicles were exposed and injected directly with MuVSEL cells isolated from GFP transgenic mice. *Bottom:* BMSCs infected with AdBMP7 were coinjected with MuVSEL cells isolated from GFP-expressing mice. At 12 months, all ossicles were recovered, decalcified, and stained with an antibody to GFP. **(B)** Staining for GFP expression in decalcified ossicles recovered BMSC/AdBMP7-implanted animals (*left*), from BMSC/AdBMP7-implanted animals, which after 1 month were exposed and injected with GFP-VSEL cells (*middle*), or ossicles established with BMSC/AdBMP7 that also contained GFP-VSEL cells at the time of implantation (*right*). Staining used anti-GFP HRP-AEC (*red*), counterstained with H&E (*light blue*). Little to no specific immunostaining for GFP was observed when the ossicles were not exposed to GFP-VSEL cells (*left*). Abundant staining of the bone marrow and bone structures were observed when the ossicles had been injected with GFP-VSEL cells. Positive staining for GFP appears in *red*. Scale bar = 100 μm. Color images available online at www.liebertpub.com/scd

cells in the serial transplantations were due almost exclusively to the aging process. The VSEL cells used in this study were derived from mice that were 6–8 weeks old. Thus, after two rounds of transplantation, the VSEL cells could have been as old as 8 months. Previous studies have demonstrated that VSEL cell loss occurs with increasing age [39]. Moreover, the serial transplant studies were performed in immunocompetent mice. We are now aware that GFP is immunogenic, and perhaps, this is, in part, why it was not possible to recover VSEL cells after the second transplantation [40]. These studies will be repeated in immunodeficient animals. It is also quite relevant to consider that context matters considerably in the systems used to identify stem cell activity, and therefore, the door should remain open before VSEL cells are defined as stem or progenitor cells. [41–43]. In fact, there are examples in the adult stem cell field where serial transplantation has not successfully been used to define stem cells [44].

In summary, to treat the complex and multitissue regenerative challenges inherent in tissue and organ repair, the identification of therapies or cells with inherent plasticity would be most desirable. VSEL cells represent an endogenous cellular population that is readily mobilized in response to wounds and can be isolated from a number of

Table 4. Retrospective Analysis of Very Small Embryonic-Like Cell Teratomas or Tumor Formation

	N =	*Duration (months)*	*Tumor/teratoma formation (%)*
HuVSEL	190	3	0
MuVSEL	35	3–12	0
Negative Control	34	3–12	0
Positive Control	110	1.5	90

Animals implanted with either human or mouse VSEL cells were evaluated for the presence of teratoma or tumor formation following endpoints of the study. At no point were teratomas or other tumors observed in any of the VSEL cell-implanted animals. Animals implanted with human prostate (PC3) or breast (MCF7) cancer cell lines (20,000 cells/injection) served as the positive control.

tissue sources. In the present study, we demonstrate that both HuVSEL and MuVSEL cells are capable of multilineage cellular differentiation in vitro. In vivo, multiple donor-derived tissue lineages, including endothelial cells, nerves, adipocytes, chondrocytes, and hematopoietic cells, were observed to be derived from HuVSEL cells, in addition to our previous demonstration of osteoblasts. These observations suggest that VSEL cells are safe and may be potentially useful therapeutic tools for tissue regeneration.

Acknowledgments

This work is directly supported by the National Institute of Health (AR0568903, DE022493, Rodgerson and Taichman; DK082481, Krebsbach and Taichman). The authors acknowledge the technical assistance provided by Gregory Yavanian, and Elizabeth Leary (NeoStem, Inc., New York, New York).

Author Disclosure Statement

D.O'N., Y.J., and D.R. are employees of NeoStem, Inc. D.R. holds stock in NeoStem, Inc. A.M.H., Y.S.,Y.J., J.W., A.M., P.H.K., R.S.T. and D.O.R. are co-inventors on a patent pending on the subject matter, which is exclusively licensed to Neostem, Inc.

References

1. Nakamura M and H Okano. (2013). Cell transplantation therapies for spinal cord injury focusing on induced pluripotent stem cells. Cell Res 23:70–80.
2. Priori SG, C Napolitano, E Di Pasquale and G Condorelli. (2013). Induced pluripotent stem cell-derived cardiomyocytes in studies of inherited arrhythmias. J Clin Invest 123:84–91.
3. Ye L, C Swingen and J Zhang. (2013). Induced pluripotent stem cells and their potential for basic and clinical sciences. Curr Cardiol Rev 9:63–72.
4. Wang Z, J Song, RS Taichman and PH Krebsbach. (2006). Ablation of proliferating marrow with 5-fluorouracil allows partial purification of mesenchymal stem cells. Stem Cells 24:1573–1582.
5. Taichman RS, Z Wang, Y Shiozawa, Y Jung, J Song, A Balduino, J Wang, LR Patel, A Havens, et al. (2010). Prospective identification and skeletal localization of cells capable of multi-lineage differentiation in vivo. Stem Cells Dev 19:1557–1570.
6. Kucia M, M Halasa, M Wysoczynski, M Baskiewicz-Masiuk, S Moldenhawer, E Zuba-Surma, R Czajka, W Wojakowski, B Machalinski and MZ Ratajczak. (2007). Morphological and molecular characterization of novel population of CXCR4+ SSEA-4+ Oct-4+ very small embryonic-like cells purified from human cord blood: preliminary report. Leukemia 21:297–303.
7. Kucia M, R Reca, FR Campbell, E Zuba-Surma, M Majka, J Ratajczak and MZ Ratajczak. (1920). A population of very small embryonic-like (VSEL) CXCR4(+)SSEA-1(+) Oct-4+ stem cells identified in adult bone marrow. Leukemia 20:857–869.
8. Kucia M, EK Zuba-Surma, M Wysoczynski, W Wu, J Ratajczak, B Machalinski and MZ Ratajczak. (2007). Adult marrow-derived very small embryonic-like stem cells and tissue engineering. Expert Opin Biol Ther 7:1499–1514.
9. Kucia MJ, M Wysoczynski, W Wu, EK Zuba-Surma, J Ratajczak and MZ Ratajczak. (2008). Evidence that very small embryonic-like stem cells are mobilized into peripheral blood 7. Stem Cells 26:2083–2092.
10. Liu Y, L Gao, EK Zuba-Surma, X Peng, M Kucia, MZ Ratajczak, W Wang, V Enzmann, HJ Kaplan and DC Dean. (2009). Identification of small Sca-1(+), Lin(−), CD45(−) multipotential cells in the neonatal murine retina. Exp Hematol 37:1096–1107.
11. Ratajczak MZ, B Machalinski, W Wojakowski, J Ratajczak and M Kucia. (2007). A hypothesis for an embryonic origin of pluripotent Oct-4(+) stem cells in adult bone marrow and other tissues. Leukemia 21:860–867.
12. Kucia M, J Ratajczak, R Reca, A Janowska-Wieczorek and MZ Ratajczak. (2004). Tissue-specific muscle, neural and liver stem/progenitor cells reside in the bone marrow, respond to an SDF-1 gradient and are mobilized into peripheral blood during stress and tissue injury. Blood Cells Mol Dis 32:52–57.
13. Ratajczak MZ, DM Shin, J Ratajczak, M Kucia and A Bartke. (2010). A novel insight into aging: are there pluripotent very small embryonic-like stem cells (VSELs) in adult tissues overtime depleted in an Igf-1-dependent manner? Aging (Albany NY) 2:875–883.
14. Kucia M, R Reca, FR Campbell, E Zuba-Surma, M Majka, J Ratajczak and MZ Ratajczak. (2006). A population of very small embryonic-like (VSEL) CXCR4(+)SSEA-1(+)Oct-4+ stem cells identified in adult bone marrow. Leukemia 20:857–869.
15. Havens AM, Y Shiozawa, Y Jung, H Sun, J Wang, S McGee, A Mishra, LS Taichman, T Danciu, et al. (2013). Human very small embryonic-like cells generate skeletal structures, in vivo. Stem Cells Dev 22:622–630.
16. Krebsbach PH, K Gu, RT Franceschi and RB Rutherford. (2000). Gene therapy-directed osteogenesis: BMP-7-transduced human fibroblasts form bone in vivo. Hum Gene Ther 11:1201–1210.
17. Franceschi RT, D Wang, PH Krebsbach and RB Rutherford. (2000). Gene therapy for bone formation: in vitro and in vivo osteogenic activity of an adenovirus expressing BMP7. J Cell Biochem 78:476–486.
18. Pelosi E, G Castelli and U Testa. (2012). Human umbilical cord is a unique and safe source of various types of stem cells suitable for treatment of hematological diseases and for regenerative medicine. Blood Cells Mol Dis 49:20–28.
19. Sovalat H, M Scrofani, A Eidenschenk, S Pasquet, V Rimelen and P Henon. (2011). Identification and isolation from either adult human bone marrow or G-CSF-mobilized

peripheral blood of CD34(+)/CD133(+)/CXCR4(+)/Lin(−)CD45(−) cells, featuring morphological, molecular, and phenotypic characteristics of very small embryonic-like (VSEL) stem cells. Exp Hematol 39:495–505.
20. Kennea NL and H Mehmet. (2002). Transdifferentiation of neural stem cells, or not? Pediatr Res 52:320–321.
21. Tsai RY, R Kittappa and RD McKay. (2002). Plasticity, niches, and the use of stem cells. Dev Cell 2:707–712.
22. Balsam LB, AJ Wagers, JL Christensen, T Kofidis, IL Weissman and RC Robbins. (2004). Haematopoietic stem cells adopt mature haematopoietic fates in ischaemic myocardium. Nature 428:668–673.
23. Mezey E. (2004). Commentary: on bone marrow stem cells and openmindedness. Stem Cells Dev 13:147–152.
24. Lee KS, HJ Kim, QL Li, XZ Chi, C Ueta, T Komori, JM Wozney, EG Kim, JY Choi, HM Ryoo and SC Bae. (2000). Runx2 is a common target of transforming growth factor beta1 and bone morphogenetic protein 2, and cooperation between Runx2 and Smad5 induces osteoblast-specific gene expression in the pluripotent mesenchymal precursor cell line C2C12. Mol Cell Biol 20:8783–8792.
25. Matsubara T, K Kida, A Yamaguchi, K Hata, F Ichida, H Meguro, H Aburatani, R Nishimura and T Yoneda. (2008). BMP2 regulates Osterix through Msx2 and Runx2 during osteoblast differentiation. J Biol Chem 283:29119–29125.
26. Ichikawa K, N Mimura and A Asano. (1993). Brefeldin A inhibits muscle-specific gene expression during differentiation in C2C12 myoblasts. Exp Cell Res 209:333–341.
27. Burattini S, P Ferri, M Battistelli, R Curci, F Luchetti and E Falcieri. (2004). C2C12 murine myoblasts as a model of skeletal muscle development: morpho-functional characterization. Eur J Histochem 48:223–233.
28. Miyanishi M, Y Mori, J Seita, JY Chen, S Karten, CK Chan, H Nakauchi and IL Weissman. (2013). Do pluripotent stem cells exist in adult mice as very small embryonic stem cells? Stem Cell Rep 1:198–208.
29. Danova-Alt R, A Heider, D Egger, M Cross and R Alt. (2012). Very small embryonic-like stem cells purified from umbilical cord blood lack stem cell characteristics. PLoS One 7:e34899.
30. Szade K, K Bukowska-Strakova, WN Nowak, A Szade, N Kachamakova-Trojanowska, M Zukowska, A Jozkowicz and J Dulak. (2013). Murine bone marrow Lin(−)Sca(−)1(+)CD45(−) very small embryonic-like (VSEL) cells are heterogeneous population lacking Oct-4A expression. PLoS One 8:e63329.
31. Kassmer SH and DS Krause. (2013). Very small embryonic-like cells: biology and function of these potential endogenous pluripotent stem cells in adult tissues. Mol Reprod Dev 80:677–690.
32. Anand S, D Bhartiya, K Sriraman, H Patel, D Manjramkar, G Bakshi, V Dhamankar and P Kurkure. (2013). Quiescent very small embryonic-like stem cells resist oncotherapy and can restore spermatogenesis in germ cell depleted mammalian testis. Stem Cells Dev [Epub ahead of print]; DOI:10.1089/scd.2013.0059.
33. Bhartiya D, S Kasiviswananthan and A Shaikh. (2012). Cellular origin of testis-derived pluripotent stem cells: a case for very small embryonic-like stem cells. Stem Cells Dev 21:670–674.
34. Ratajczak MZ, E Zuba-Surma, W Wojakowski, M Suszynska, K Mierzejewska, R Liu, J Ratajczak, DM Shin and M Kucia. (2013). Very small embryonic-like stem cells (VSELs) represent a real challenge in stem cell biology: recent pros and cons in the midst of a lively debate. Leukemia [Epub ahead of print]; DOI: 10.1038/leu.2013.255.
35. Suszynska M, E Zuba-Surma, M Maj, K Mierzejewska, J Ratajczak, M Kucia and MZ Ratajczak. (2013). The proper criteria for identification and sorting of very small embryonic-like stem cells (VSELs), and some nomenclature issues. Stem Cells Dev [Epub ahead of print]; DOI:10.1089/scd.2013.0472.
36. Starzynska T, K Dabkowski, W Blogowski, E Zuba-Surma, M Budkowska, D Salata, B Dolegowska, W Marlicz, J Lubikowski and MZ Ratajczak. (2013). An intensified systemic trafficking of bone marrow-derived stem/progenitor cells in patients with pancreatic cancer. J Cell Mol Med 17:792–799.
37. Kucia M, M Masternak, R Liu, DM Shin, J Ratajczak, K Mierzejewska, A Spong, JJ Kopchick, A Bartke and MZ Ratajczak. (2013). The negative effect of prolonged somatotrophic/insulin signaling on an adult bone marrow-residing population of pluripotent very small embryonic-like stem cells (VSELs). Age (Dordr) 35:315–330.
38. Ratajczak J, M Wysoczynski, E Zuba-Surma, W Wan, M Kucia, MC Yoder and MZ Ratajczak. (2011). Adult murine bone marrow-derived very small embryonic-like stem cells differentiate into the hematopoietic lineage after coculture over OP9 stromal cells. Exp Hematol 39:225–237.
39. Ratajczak MZ, DM Shin, R Liu, K Mierzejewska, J Ratajczak, M Kucia and EK Zuba-Surma. (2012). Very small embryonic/epiblast-like stem cells (VSELs) and their potential role in aging and organ rejuvenation—an update and comparison to other primitive small stem cells isolated from adult tissues. Aging (Albany NY) 4:235–246.
40. Bubnic SJ, A Nagy and A Keating. (2005). Donor hematopoietic cells from transgenic mice that express GFP are immunogenic in immunocompetent recipients. Hematology 10:289–295.
41. Quesenberry PJ, MS Dooner, LR Goldberg, JM Aliotta, M Pereira, A Amaral, MM Del Tatto, DC Hixson and B Ramratnam. (2012). A new stem cell biology: the continuum and microvesicles. Trans Am Clin Climatol Assoc 123:152–166; discussion 166.
42. Liu L, EF Papa, MS Dooner, JT Machan, KW Johnson, LR Goldberg, PJ Quesenberry and GA Colvin. (2012). Homing and long-term engraftment of long- and short-term renewal hematopoietic stem cells. PLoS One 7:e31300.
43. Quesenberry PJ, MS Dooner and JM Aliotta. (2010). Stem cell plasticity revisited: the continuum marrow model and phenotypic changes mediated by microvesicles. Exp Hematol 38:581–592.
44. Christ B and S Pelz. (2013). Implication of hepatic stem cells in functional liver repopulation. Cytometry A 83:90–102.

Address correspondence to:
Dr. Russell S. Taichman
Department of Periodontics and Oral Medicine
University of Michigan School of Dentistry
1011 North University Avenue
Ann Arbor, MI 48109-1078

E-mail: rtaich@umich.edu

Received for publication August 2, 2013
Accepted after revision December 28, 2013
Prepublished on Liebert Instant Online December 29, 2013